

The Pennsylvania State University, University Park, U.S.A.

# The Role of the Convective “Trigger Function” in Numerical Forecasts of Mesoscale Convective Systems

J. S. Kain and J. M. Fritsch

With 7 Figures

Received November 18, 1991

Revised April 27, 1992

## Summary

Three-dimensional numerical model simulations of a mesoscale convective system are performed to evaluate the sensitivity of the simulations to differences in the convective trigger function. The Penn State/NCAR mesoscale model with the Kain-Fritsch convective parameterization scheme is used as the modeling system for the study. All simulations are performed on the June 10–11, 1985 squall line from the OK PRE-STORM field experiment. Individual simulations differ only in their specification of the trigger function within the Kain-Fritsch scheme. Comparison of results from 12 hour simulations indicates that the position, timing, and intensity of convective activity and mesoscale features vary substantially as a function of the trigger function formulation. The results suggest that the convective trigger function is an integral part of the overall convective parameterization problem, and that great care must be exercised in designing realistic trigger function formulations, especially as model resolutions approach the scale of individual convective clouds.

## 1. Introduction

Convective parameterization is an important and well known problem that has confronted the numerical modeling community for many years. Early convective parameterization theories and procedures were designed for synoptic and global scale models in which the grid elements were so large (e.g.,  $\Delta X \sim 500$  km) that they encompassed entire mesoscale convective systems. For such coarse resolution, it was impossible and unneces-

sary to know the location and configuration of active convective cells that comprised mesoscale convective systems. Consequently, convective parameterization techniques typically relied on empirically-based relationships between observed larger-scale processes and convective activity to predict when and where convection should occur. For example, some parameterizations were designed to initiate convection when a threshold value of mass or moisture convergence was exceeded at a grid point where the atmosphere was conditionally unstable (e.g., Kuo, 1974). Others operated under the assumption of a state of “quasi-equilibrium” between convective scale and larger scale processes so that they initiated convection when the model atmosphere tended to deviate too far from some assumed or calculated equilibrium state (e.g., Arakawa and Schubert, 1974 [AS]).

More recent models have much finer resolution (e.g.,  $\Delta X \sim 25$  km) and explicitly simulate many of the *mesoscale* features that can play a major role in determining when and where convection will occur. Conceptually then, they are capable of resolving much more accurately the locations of convective activity. However, because parameters such as grid-scale convergence and destabilization rate are governed by different dynamical constraints on these scales, and because there is a dearth of supporting observational evidence on

these scales, it is not clear that larger scale relationships between resolvable scale dynamical processes and convective activity are sufficient predictors of deep convection at these grid resolutions. For this reason, when parameterization closures based on larger scale dynamical tendencies are used in *mesoscale* models, additional criteria are often imposed in evaluating the potential for convective initiation.

These criteria are usually designed to reflect some measure of the accessibility of potential buoyant energy, or the probability of parcels reaching their level of free convection (LFC) in a conditionally unstable atmosphere. These additional constraints are appropriate because the onset of deep convection in a given vertical column is often strongly modulated by the strength of a capping stable layer beneath the LFC. For example, the Anthes-Kuo scheme (Anthes, 1977), as used in the Penn State/NCAR mesoscale model, allows convection only when the negative area for pseudo-adiabatic ascent (on a thermodynamic diagram) becomes less than the positive area; the AS scheme, as used by Grell (1991), does not allow convection until the lifting required for parcels to reach their level of free convection becomes less than some specified depth (Grell, personal communication).

In some schemes designed specifically for mesoscale models (i.e., Kreitzberg and Perkey, 1976; Fritsch and Chappell, 1980 [FC]; Frank and Cohen, 1985; Kain and Fritsch, 1990 [KF]), the ability of rising parcels to reach their LFC is estimated using parcel theory and the buoyancy equation. In order to overcome a layer of negative buoyancy below the LFC, air parcels must typically have some positive vertical velocity and/or hydrothermal perturbation. The magnitude of this perturbation can be either assigned a constant value to be used at all grid points (as in Kreitzberg and Perkey as well as Frank and Cohen) or related in some way to resolvable-scale dynamical tendencies (as in FC and KF). Although there is some evidence that perturbation values can be related to mesoscale forcing (e.g., Chen and Orville, 1980), a firm quantitative link between the two has not yet been established. Indeed, even numerical investigations using cloud scale (i.e.  $\Delta X \sim 1-2$  km) models typically rely on artificial imposition of random hydrothermal perturbations to initiate deep convection.

The complete set of criteria used to determine when and where deep convection occurs in a numerical model is collectively termed the convective “trigger function”. The purpose of this paper is explore the sensitivity of numerical simulations of the structure and evolution of a particular mesoscale convective system to the specific formulation of the convective trigger function. In the following section, the numerical modeling system used in the sensitivity experiments is briefly described and the different trigger function formulations are presented. Section 3 describes the results of the numerical experiments, and section 4 discusses the implications of the results in the general context of the cumulus parameterization problem.

## 2. Methodology

Different trigger function formulations are investigated by varying the convective initiation criteria within a single convective parameterization scheme. Sensitivities are demonstrated through fully prognostic numerical simulations of a mesoscale convective system.

### 2.1 Numerical Modeling System

The numerical model used for this study is the Pennsylvania State University/National Center for Atmospheric Research (PSU/NCAR) mesoscale model (Anthes and Warner, 1978; Anthes et al., 1987). The model configuration and physical parameterizations are very similar to the setup used by Zhang et al. (1989), including

- A two-way interactive nested grid (Zhang et al., 1986) with coarse grid resolution of 75 km and fine grid resolution of 25 km;
- Explicit prediction of precipitation processes, including predictive equations for cloud water, cloud ice, rain water, and snow (Zhang, 1989; Dudhia, 1989);
- Anthes and H. L. Kuo (Anthes, 1977; Kuo 1974) parameterization of deep convection on the coarse grid only;
- A high resolution Blackadar (1979) planetary boundary layer parameterization (Zhang and Anthes, 1982; Zhang and Fritsch, 1986).

The present model physics package differs most significantly from that of Zhang et al. (1989) in its implicit parameterization of moist convection. The

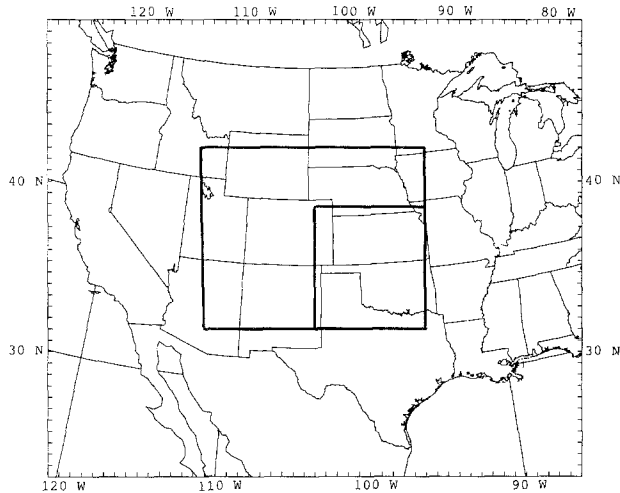


Fig. 1. Coarse-grid domain for numerical simulations. First inset is the fine-grid domain, second inset indicates the area over which the results are presented

FC convective parameterization scheme, used only on the higher resolution grid by Zhang et al. has been replaced by the KF scheme. Although the KF scheme relies on the same basic closure assumptions as FC, it utilizes more sophisticated representations of cloud-environment interactions and imposes rigorous constraints on mass, moisture, and energy conservation, among other more subtle differences.

The model uses a terrain-following sigma vertical coordinate with 19 vertical levels on both coarse and fine grids. The horizontal dimensions of the grids are  $49 \times 41$  for the coarse resolution and  $61 \times 49$  for the fine resolution. The coarse mesh domain covers most of the continental United States west of the Appalachians, while the higher resolution domain covers an area near the center of this region, as shown in Fig. 1. Also indicated is an area in the southeastern part of the fine mesh domain over which model results for this study will be presented.

## 2.2 Trigger Function Formulations

The convective trigger function for a given numerical model is defined by the set of criteria used to initiate parameterized convection. For the present study, five trigger functions were selected for testing. Listed below are brief descriptions of the different function formulations.

### 2.2.1 Original Fritsch-Chappell Trigger (FCT)

The trigger function used in the original FC scheme is based on observational and numerical modeling evidence that the size and strength of boundary layer hygrotherms that act as the “roots” of incipient convective clouds are a function of the strength of larger-scale boundary layer convergence (Bean et al., 1972, 1975; Chen and Orville, 1980). Specifically, FC related sub-grid scale temperature perturbations ( $\delta T$ ) to the model resolvable scale vertical velocity ( $w_0$ ) at the lifting condensation level (LCL) such that  $\delta T \propto w_0^{1/3}$ , where  $\delta T$  and  $w_0$  have units of K and  $\text{m s}^{-1}$ , respectively. The current application is performed in a manner similar to FC. Beginning with the model layer closest to the ground, the thermodynamic properties of adjacent layers overhead are mixed in a mass-weighted fashion until the combined depth of the mixture,  $\delta p_m$ , is at least 60 hPa (the actual depth is a function of the depth of the individual layers). The mixture is “lifted” to its LCL where its temperature and pressure are calculated. If the sum of the mixture’s LCL temperature plus  $\delta T$  is greater than the grid-scale temperature at that level, the buoyancy equation is used to estimate whether this perturbation is strong enough to allow the parcel to reach its LFC. If not, a similar mixture of layers beginning with the second-lowest layer is checked in the same way, and so on, until a buoyant mixture is found or each layer in the lowest 300 hPa has been tested.

### 2.2.2 Anthes-Kuo Type Trigger (AKT)

This trigger function is nearly identical to that used in the Anthes-Kuo convective parameterization as it is applied in the PSU/NCAR mesoscale model. For a cloud to be triggered, three criteria must be satisfied:

- Column integrated moisture convergence must exceed a specified threshold value (default value set at  $3.0 \times 10^{-5} \text{ kg m}^{-2} \text{ s}^{-1}$  in the Penn State/NCAR mesoscale model).
- The positive area below cloud top on a thermodynamic diagram must be greater than the negative area. The positive area is computed for the mixture ( $\delta p_m$ ) that has the highest  $\theta_e$  value in the column. The highest  $\theta_e$  value is determined from the resolvable scale temperature and water vapor mixing ratio plus 1 K and  $1 \text{ g kg}^{-1}$ , respectively.

- The cloud must have a depth of at least  $\sigma = 0.3$ , where  $\sigma = \frac{P - P_t}{P_s - P_t}$  and  $P$  is the pressure level,  $P_s$  is the surface pressure,  $P_t$  is the pressure at model top.

### 2.2.3 Negative Area Trigger (NAT)

The NAT computes the negative area on a thermodynamic diagram between the most unstable (highest  $\theta_e$ ) model layers,  $\delta p_m$ , and the LFC. The ability of a parcel from this mixture to overcome the negative area is estimated by assigning a perturbation vertical velocity based on the assumption that the resolvable-scale mass convergence is concentrated over an area comparable to the dimensions of an individual cloud. Specifically, the perturbation vertical velocity,  $w_p$ , of a rising parcel is assumed to be directly proportional to the resolvable scale vertical velocity, i.e.,  $w_p = kw_0$ , where  $k$  has a value on the order of about 10–100. If  $w_p$  is sufficiently large to maintain upward motion through the layer of negative buoyancy, a cloud is initiated.

### 2.2.4 Lifting Depth Trigger (LDT)

This trigger is similar to the NAT in that the difference in height (or pressure) between the most unstable mixture,  $\delta p_m$ , and its LFC is computed. If the difference is less than some specified depth, typically on the order of 50–250 hPa, a cloud is allowed. The significant difference between this test and NAT is that this test is not a direct function of instantaneous resolvable-scale tendencies.

The KF scheme becomes, in principle, quite similar to Grell's (1991) adaptation of the Arakawa-Schubert scheme for mesoscale models when the LDT is implemented. In Grell's application, AS's quasi-equilibrium assumption is held in abeyance until the lifting depth check suggests that potential buoyant energy can become available. At this stage, the time rate of change of the cloud work function (the cloud work function can be thought of as a measure of the convective available potential energy [CAPE]) is calculated as the sum of cloud work function at the current time step plus the change that would be brought about by extrapolating the current tendency over a convective time period (typically 30 minutes), all divided by the convective time period. Minimizing the time rate of change of the cloud work function then

essentially amounts to eliminating the CAPE in a column over the convective time period, which is the fundamental closure assumption of the FC and KF schemes. The LDT as applied in the modified AS scheme differs primarily from the current application in the FC scheme by requiring both instantaneous destabilization in a column and a minimum lifting depth for unstable layers.

### 2.2.5 Boundary Layer Forcing Check (BLT)

The BLT utilizes boundary layer theory (Stull, 1988) to estimate the perturbation vertical velocity of parcels that originate in a convective boundary layer. A mixed parcel is given a vertical velocity equal to the free convection scaling velocity,  $w_*$ , which is a function of surface buoyancy flux and the height of the planetary boundary layer. The surface buoyancy flux is given by  $\frac{g}{\theta_v} \overline{w' \theta'_v}$ , where  $\theta_v$  is the virtual potential temperature,  $g$  is the acceleration due to gravity, and the overbar indicates the mean value in a grid element. Specifically,

$$w_* = \left[ \frac{gz_i}{\theta_v} \overline{w' \theta'_v} \right]^{1/3},$$

where  $z_i$  is the height of the boundary layer. The buoyancy flux and boundary layer height are derived from the high resolution planetary boundary layer parameterization. Since this type of trigger is applicable only for parcels originating in a well-fixed boundary layer driven by surface heating, and since convective clouds are often fed from elevated sources, this trigger function is used only in combination with the FCT or NAT formulations. As in the LDT formulation, this type of trigger function is only indirectly related to instantaneous resolvable-scale dynamical forcing.

## 3. Results

The event selected for this study is the OK PRE-STORM (Oklahoma-Kansas Preliminary Regional Experiment for Stormscale Operational and Research Meteorology; see Cuning, 1986) June 10–11 1985 squall line. Initial model conditions are identical to those used by Zhang et al. (1989) and Zhang and Gao (1989) and are valid at 1200 UTC June 10, 1985 (Fig. 2).

A series of 12 hour simulations of this event were performed with the only difference between the

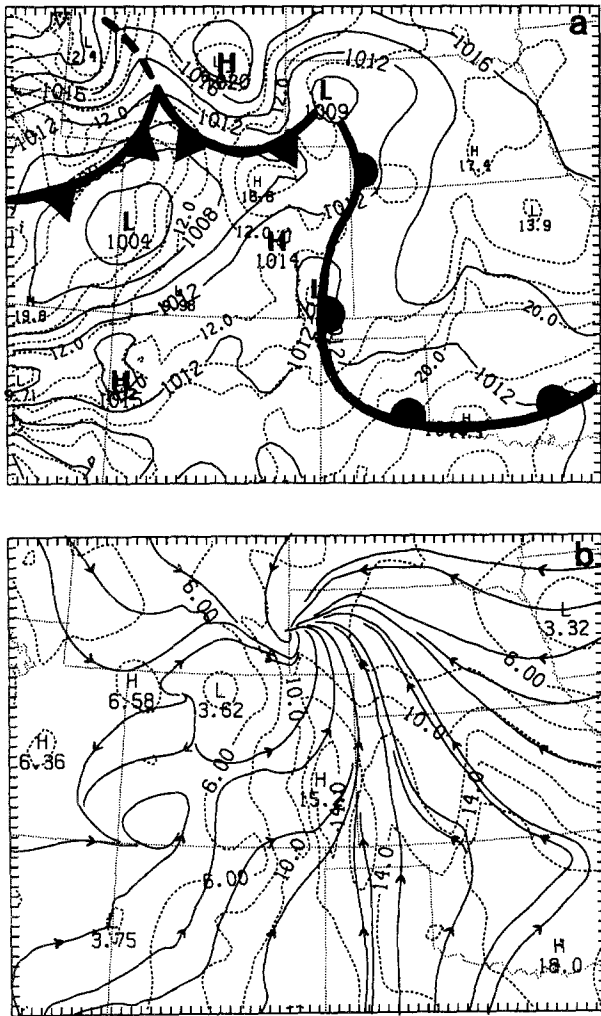


Fig. 2. Analysis of model initial surface conditions over the fine-mesh domain, valid at 1200 UTC 10 June 1985 (adapted from Zhang et al., 1989). (a) Sea-level pressure at intervals of 2 hPa (solid) and temperature at intervals of 2 K (dashed). (b) Stream line (solid), and specific humidity (dashed) at intervals of  $2 \text{ g kg}^{-1}$ .

runs being the trigger function formulation in the KF scheme. Observations and analyses of the event are also presented for comparison with modeling results so that the credibility of the modeling system may be established. However, the intended emphasis in the model results that will be shown is the variability of the solutions as a function of different convective trigger functions rather than a comparison with observations.

### 3.1 Observations

Analyses of the observations from the 9 and 12 hour times, 2100 UTC June 10 and 0000 UTC June 11, 1985, respectively, are shown in Figs.

3a, c. These analyses show three major features of particular interest for this case: 1) a mesolow near the northeastern corner of the Texas Panhandle at both times; 2) a surface cold front, extending from near the Kansas-Nebraska border just east of Colorado, towards the south-southeast across the southeastern corner of Colorado at the 9 hour time, and, at the 12 hour time, a convective outflow boundary that has run out ahead of the front, extending from central Kansas southwestward just to the northwest of the mesolow, and then west-southwestward across the Panhandle; and 3) a surface warm front, stretching from the southern Colorado-Kansas border south and east until it becomes nearly parallel to the Texas border in southern Oklahoma at the 9 hour time, and extending nearly east to west across central Oklahoma at the 12 hour time. The locations of active deep convection at these times can be inferred from Figs. 3b, d. The visible satellite image of the region at the 2101 UTC (9 hour time, Fig. 3b) shows the early stages of the the developing squall line nearly parallel to, but apparently several tens of kilometers out ahead of, the location of the surface cold front (cf. Fig. 3a). Also revealed in this image is a cloud shield associated with a decaying mesoscale convective system (MCS) over eastern Kansas. By 2320 UTC, a composite of the Amarillo and Wichita digitized WSR-57 radar reflectivity patterns (Fig. 3d) indicates a line of thunderstorms running roughly overhead and just to the rear of the analyzed position of the surface outflow boundary at 0000 UTC (cf. Fig. 3c). Also indicated by the radar at this time are regions of apparent convective activity in southeastern and north-central Kansas.

### 3.2 Model Simulations

The results obtained using the FCT in this case are shown in Fig. 4. At the 9 hour time, a broken line of convection extends from northwestern Kansas to the south-southwest and across the northwest tip of the Texas Panhandle, consistent with the satellite picture of Fig. 3b. Parameterized convection is also active over west-central and northeastern Kansas, reasonably close to the cloudy areas shown in the satellite image. However, in this model run, convection is active over a large part of the Texas Panhandle, well to the south and east of the primary mesoscale triggering

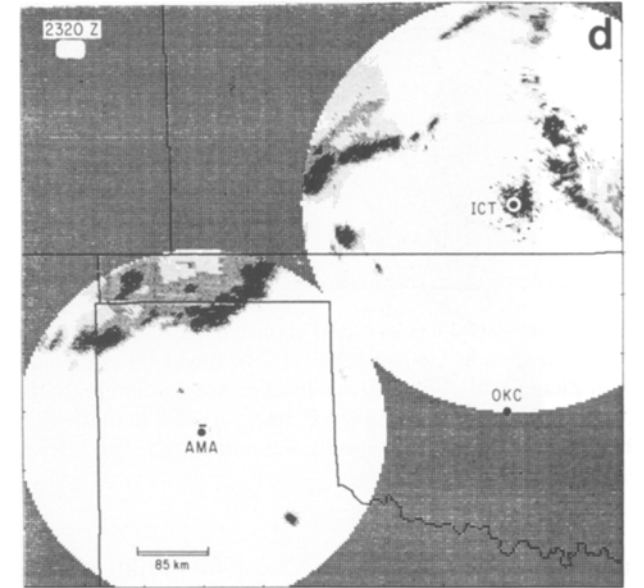
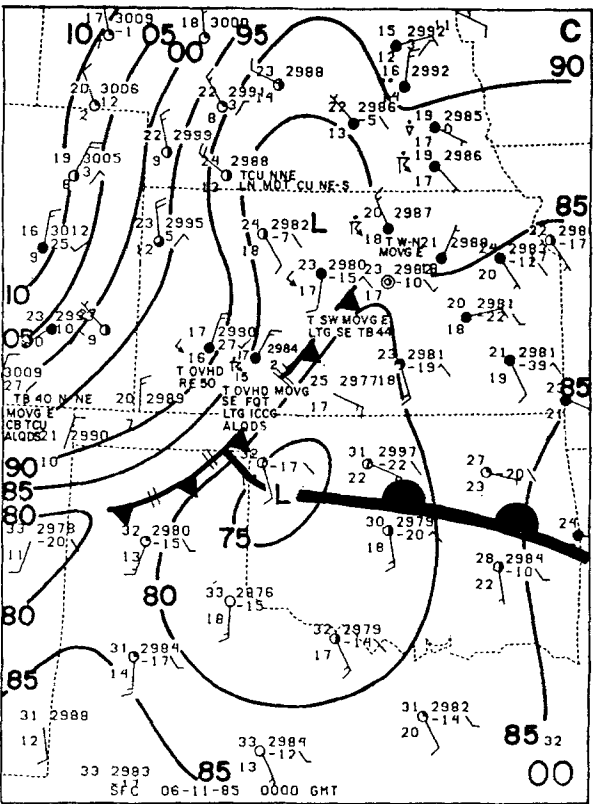
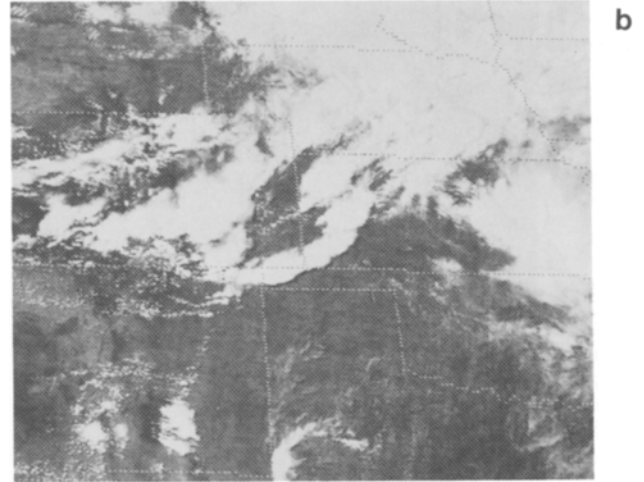
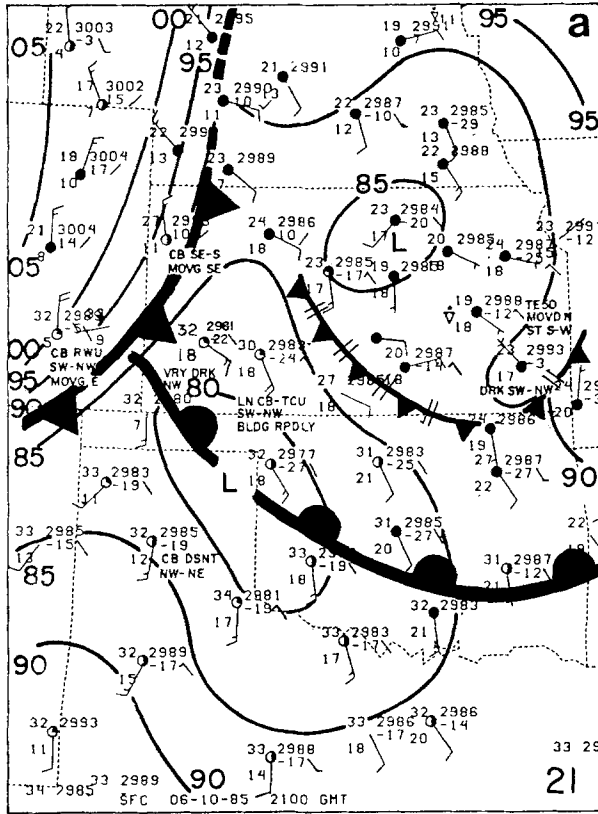


Fig. 3. Surface mesoanalysis (a) and visible satellite image (b) valid at 2100 UTC 10 June 1985; surface mesoanalysis valid at 0000 UTC 11 June 1985 (c) and composite low-level echo patterns from the AMA and ICT WSR-57 10 cm radars valid at 2320 UTC 10 June 1985 (d). Isobars are drawn for altimeter settings: units are inches of mercury, e.g., 85 = 29.85 in Hg. For wind speed, one full barb =  $5 \text{ m s}^{-1}$ , one half barb =  $2.5 \text{ m s}^{-1}$ . In (d), the composite echo patterns were formed by merging  $1^\circ$  elevation scans from these radars. Reflectivity values are 15–25 dBz, light stippling; 25–35 dBz, heavy stippling; 35–50 dBz, hatching; and > 50 dBz, solid. Parts (a), (b), and (c) are adapted from Johnson and Hamilton, 1988; part (d) is from Rutledge et al., 1988. Mesoanalysis conventions follow Young and Fritsch (1989)

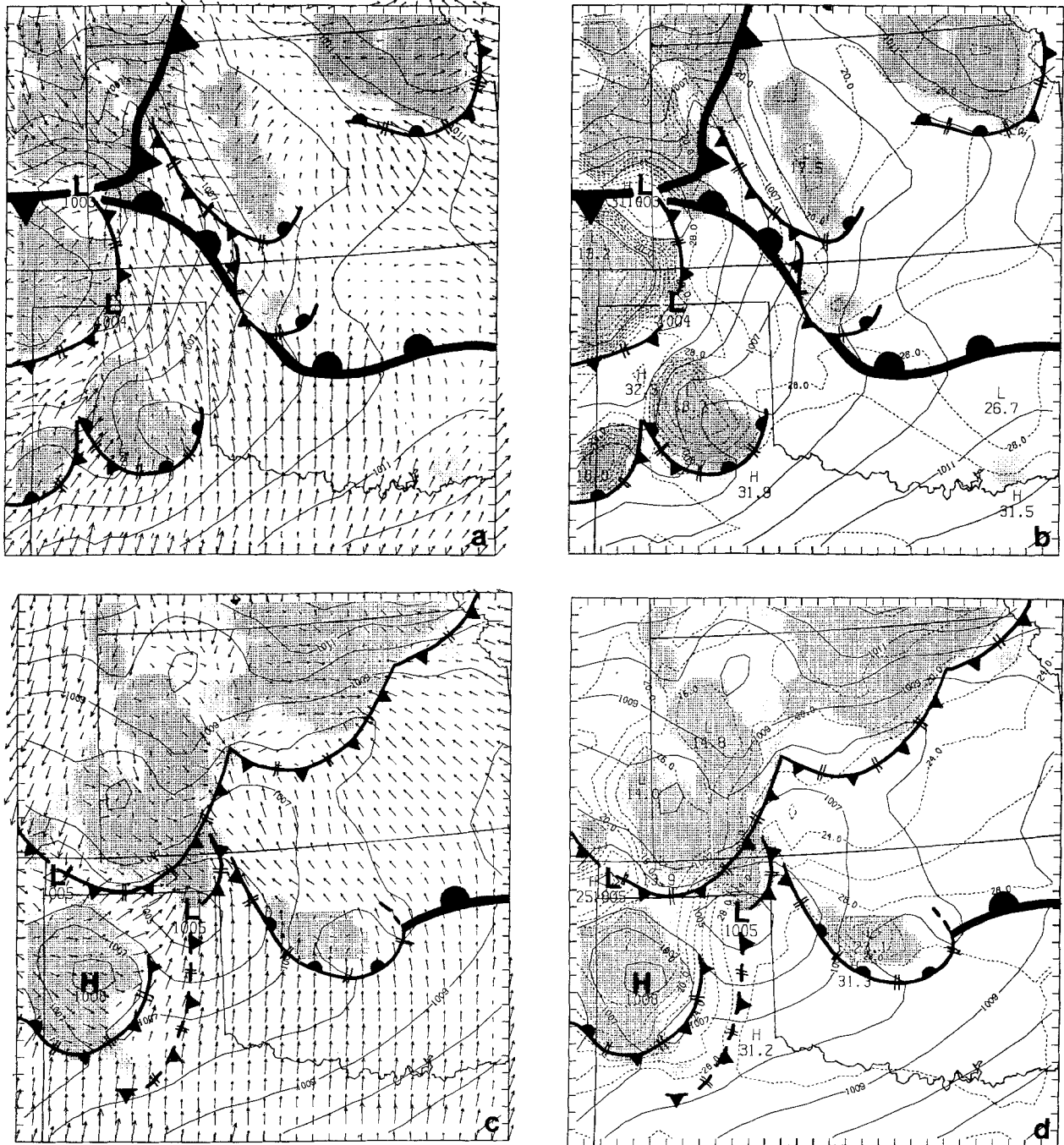


Fig. 4. Distribution of sea-level pressure (hPa) and surface wind vectors (a, c) and sea-level pressure and temperature (dashed, K) (b, d) for a 12 hour simulation using the Fritsch-Chappell type trigger (FCT) function. Parts (a) and (b) are valid at the 9 hour time and parts (c) and (d) are valid at the 12 hour time. Shading indicates areas of convective activity within the hour preceding the analysis

mechanism (i.e., the surface cold front). The surface mesolow over the northern Texas Panhandle is 50–100 km to the west of its observed location and the mesolow positioned along the Kansas-Colorado border, in between the convectively active regions, was apparently not observed by the convectational surface network. Note, however,

that the model-predicted position of the Kansas-Colorado low is very near the observed intersection point of the cold and warm fronts, a common location for low pressure centers.

At the 12 hour time, there is only one mesolow and its simulated position is only slightly to the west of its observed location. However, in contrast

to observations, new convection has broken out along the warm front in central Oklahoma. Satellite imagery (not shown) reveals building cumulus clouds in this region, but deep convection did not develop at this location until about four hours later. In addition to the premature convective development over central Oklahoma, parameterized convection continues to occur over the

western half of the Texas Panhandle, a considerable distance to the south of its observed location. Analysis of model output from earlier times indicates that convection propagated into this region during the first three hours of the simulation as fragments of convection broke away from the MCS over eastern Kansas and Oklahoma. Parameterized convection was nearly continuously regenerated

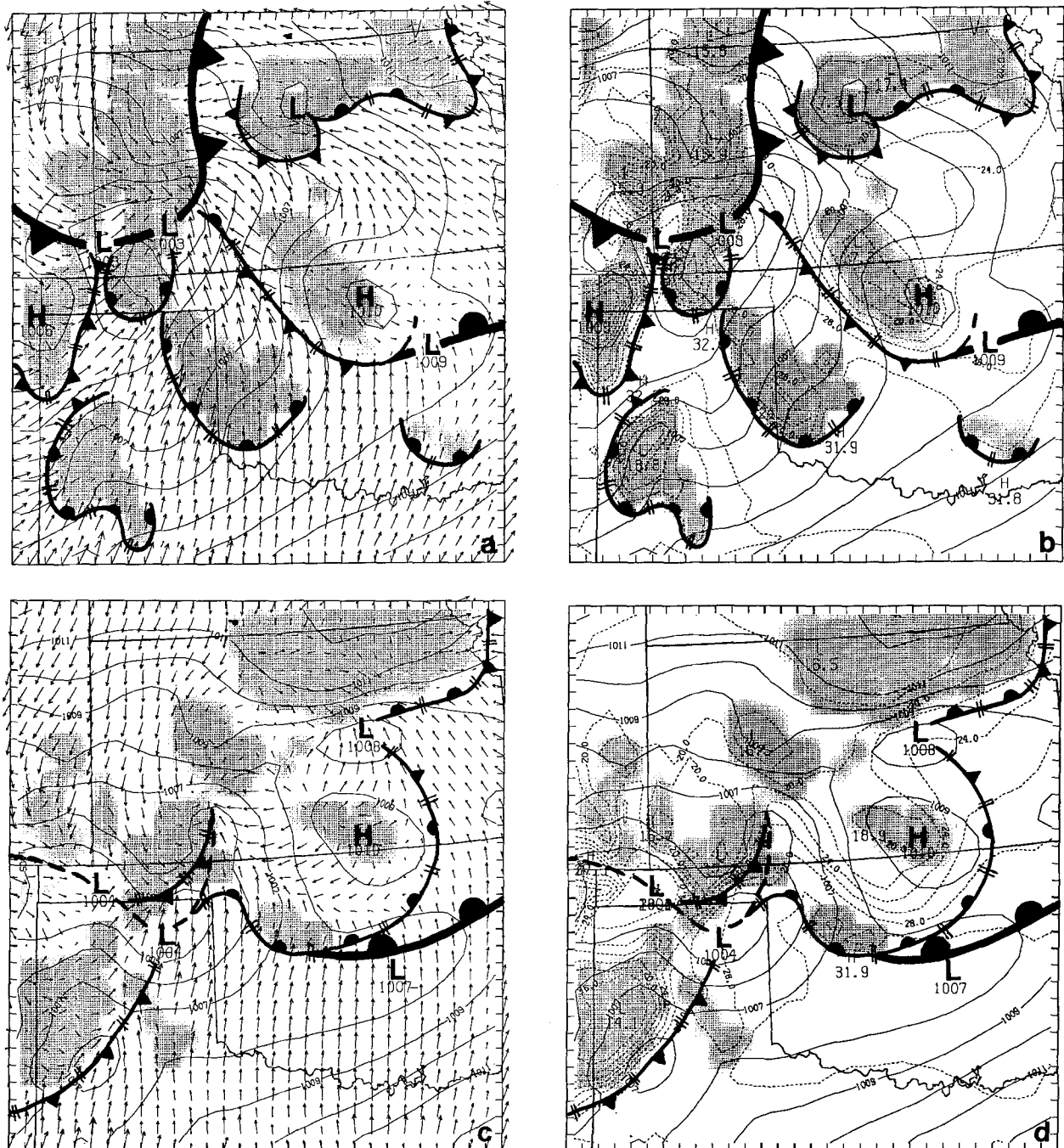


Fig. 5. As in Fig. 4, but using the Anthes-Kuo type trigger (AKT) function

in this region during the 3–12 hour time period. In spite of the localized inconsistencies, it is evident that the model does well in reproducing the main squall line structure that extends from northeastern Kansas southwestward to the Texas Panhandle.

Results of a simulation of this case using the AKT, with the moisture convergence threshold set at  $3.0 \times 10^{-4} \text{ kg m}^{-2} \text{ s}^{-1}$  (an order of magnitude larger than the default value) are shown in Fig. 5. Comparison of Figs. 4 and 5 reveals a number of similarities between the AKT and FCT simulations. As in the FCT run, at the 9 hour time (Figs. 5a, b), a line of convective storms stretches from north to south across western Kansas and into the northern tip of the Texas Panhandle. In addition, convective activity is occurring in a southwest-northeast swath stretching from the Texas Panhandle through north-central Oklahoma into central and north-eastern Kansas. Note, however, that convection is more widespread over north-central and western Oklahoma than in the FCT run. Furthermore, the structure of the mesolow differs from the FCT run in that the center is more diffuse and a lobe of lower pressure extends eastward from the mesolow center along the Kansas-Colorado border.

Three hours later in the simulation (Figs. 5c, d), the central pressure and location of the main mesolow is about the same as in the FCT run, and convection is active over the western half of the Texas Panhandle in each simulation. A readily apparent difference between the two runs is that a mesohigh-mesolow couplet with a pronounced cold pool has developed in association with active convection over Kansas in the AKT run, while no such couplet is evident in the FCT simulation (or in the observations).

A noteworthy characteristic of the execution of the AKT in this case is not obvious from the results of the simulation. Specifically, the present results differ only slightly from a simulation using the AKT with the moisture convergence threshold set an order of magnitude smaller. Furthermore, periodic checks of the input parameters used by this trigger function during the course of the simulation revealed that, even with the relatively high threshold value, the specified moisture convergence threshold was exceeded at nearly every grid point where moisture convergence was positive. These results suggest that the *sign* of moisture convergence was more of a controlling factor than

its magnitude, and that the negative area and cloud depth checks in the AKT played an important role in determining when convection would occur at grid points where moisture convergence was positive.

The simulation using the lifting depth trigger (LDT), with maximum allowable lifting required to reach the LFC set at 100 hPa, produces considerably different mesoscale features than the FCT and AKT runs in some areas of the domain. For example, nine hours into the simulation (cf. Figs. 4a, b; 5a, b; 6a, b), there is no active convection from the Texas Panhandle northward to extreme northwestern Kansas and no sign of squall line development in that region. In addition, the main mesolow center is located farther to the east. As an apparent consequence of the absence of convection over Colorado and the shift in the mesolow, the winds over the region from the Oklahoma Panhandle into west-central Kansas have a much stronger westerly component than in either the FCT or the AKT simulations. This wind shift has led to the development of a relatively strong convergence zone along the outflow boundary in south-central Kansas. In the FCT and AKT simulations, the flow was nearly parallel to boundaries in that area, implying considerably weaker convergence and convective forcing.

At the 12 hour time in the LDT simulation, the mesolow is farther to the north and the pressure gradient immediately surrounding the low is very diffuse compared to the FCT and AKT simulations (cf. Figs. 4c, d; 5c, d; 6c, d). There is no convection over extreme southwestern Kansas nor the Oklahoma and Texas Panhandle region where the squall line was observed. In addition, the meso-high-mesolow couplet over Kansas appears to have developed more slowly than in the AKT run. Of particular interest is the fact that the area of convection that was located in central Kansas at the 9 hour time has propagated southwestward into the convergence zone set up by the ambient southwesterly flow and the moist downdraft outflow. Clearly, the different trigger function changed the patterns of convective development early in this simulation, leading to nonlinear changes in the subsequent evolution of events.

Another significant feature in this simulation is the formation of an intense cold pool and associated cold outflow boundary over southeastern Colorado in the absence of parameterized deep

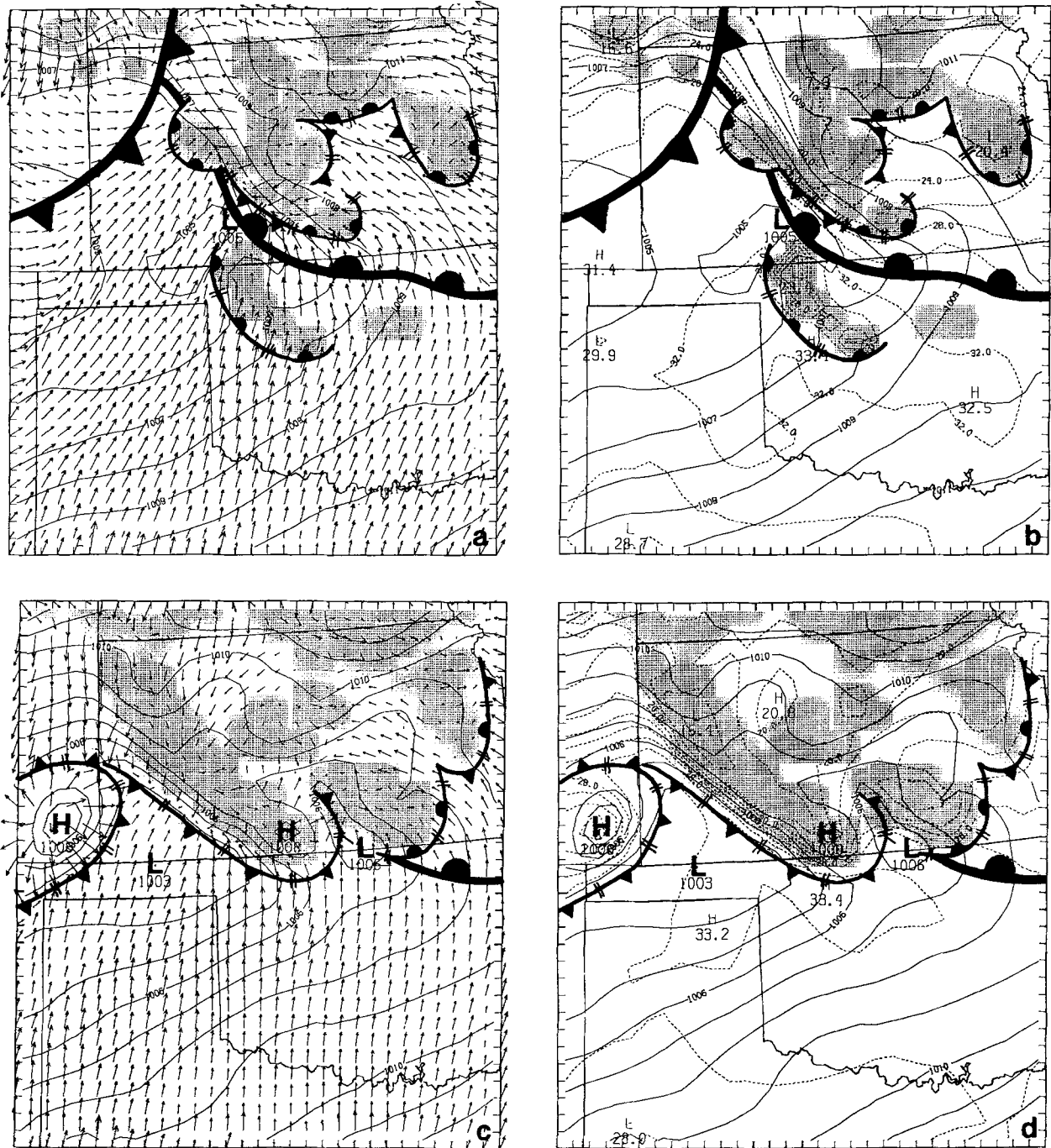


Fig. 6. As in Fig. 4, but using the lifting depth trigger (LDT) function

convection (and convective-scale downdrafts). This cold pool is generated in the model entirely through the evaporation of resolvable-scale precipitation in a very dry boundary layer. In this case, resolvable scale precipitation is generated in a conditionally unstable environment because the trigger function does not allow parameterized convection to develop. More specifically, the

thermodynamic profile in this environment is characterized by a nearly well-mixed boundary layer approximately 250 hPa deep overlain by a very moist conditionally unstable layer. The lowest model layer contains the air with the highest  $\theta_e$  value but this air must be lifted to the top of the boundary layer before reaching its LFC. Since this lifting depth exceeds the 100 hPa maximum

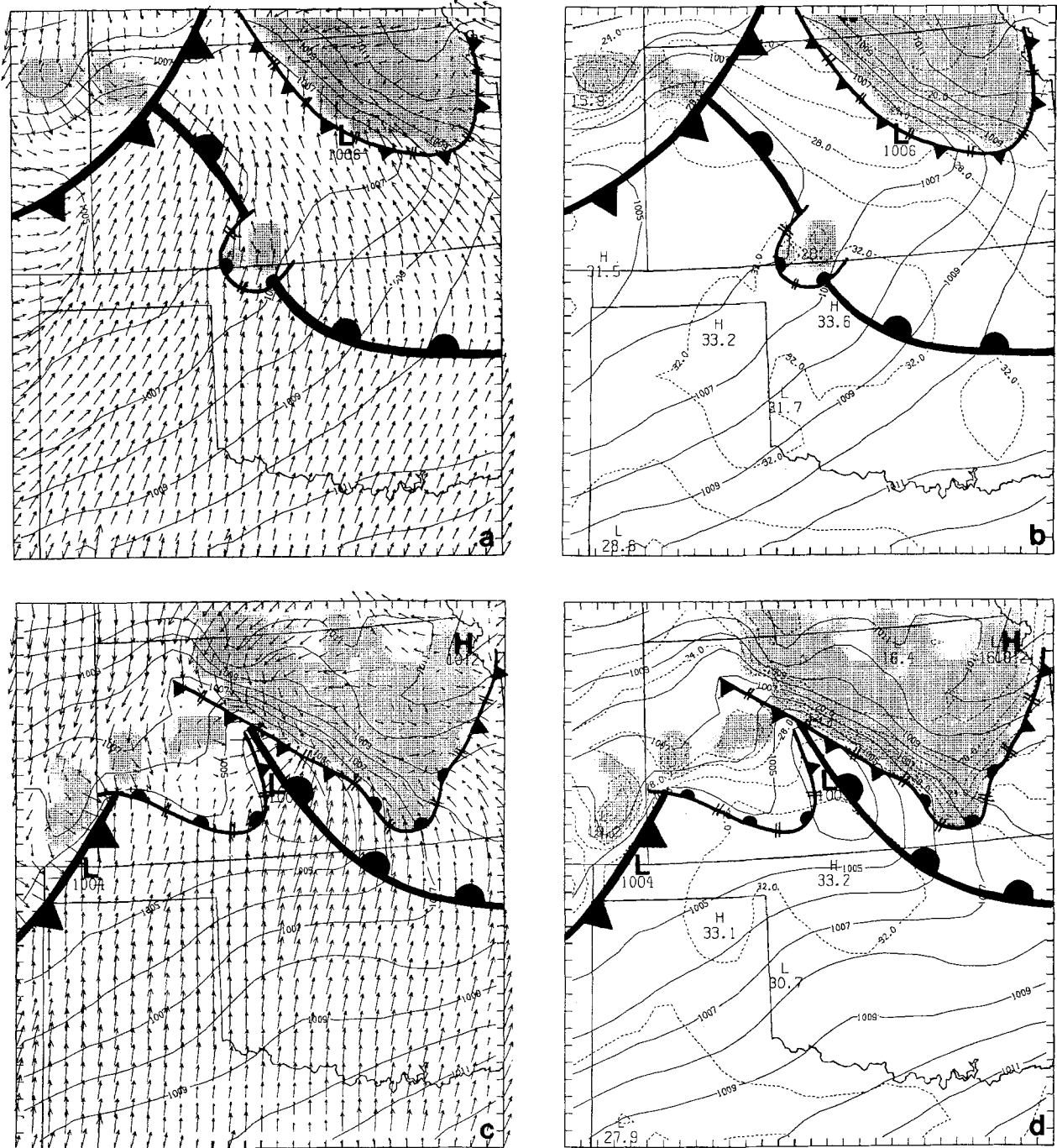


Fig. 7. As in Fig. 4, but using the negative area trigger (NAT) in combination with the boundary layer trigger (BLT)

imposed in this run, parameterized convection is not allowed and eventually saturation is achieved on the resolvable scale as air ascends out ahead the advancing short-wave trough.

The negative area check (NAT) trigger, with  $k = 10$ , was used in combination with the boundary layer check (BLT) trigger to generate the results shown in Fig. 7. At the 9 hour time, convection is

active over most of the northeastern quadrant of Kansas; a broken line of the convection, which may be the early stages of a squall line, is oriented west to east from eastern Colorado into northwestern Kansas; and a small area of convection is active along the central Kansas-Oklahoma border. In general however, the areal coverage of convection is substantially less than in the previous

three runs (cf. Figs. 4a, b; 5a, b; 6a, b). There is no evidence of a mesolow in the Texas-Oklahoma Panhandle region and no extended convective outflow boundary in west-central and south-central Kansas. In the absence of convective activity over east-central Kansas, the mesoscale trough in this region is more intense than in any of the other three simulations. As in the LDT simulation, the relatively weak convection along the Colorado-Kansas border and the failure of the mesolow to develop appear to lead to significantly stronger westerly components in the surface winds in the Panhandle region and across southwestern Kansas than in the FCT or AKT simulations.

At the 12 hour time, convection is active over much of the northeastern half of Kansas, with a mesoscale outflow boundary running diagonally from northwest to southeast across the state. Again, as in the LDT simulation, relatively strong convergence has developed along this boundary. The major mesolow is located in south-central Kansas, not the Texas-Oklahoma Panhandle region as in the other simulations, and sea-level-pressure values near the mesolow center differ from those of the other runs by as much as 5 hPa. The mesohigh that develops over south-central Kansas in the AKT and LDT simulations has not materialized and the squall line, although clearly evident, is much weaker and slower than in the FCT and AKT simulations.

#### 4. Summary and Discussion

In general, the simulations of convectively-generated mesoscale patterns for the June 10–11 case show considerable sensitivity to the formulation of the trigger function in the KF parameterization scheme. The processes associated with this sensitivity appear to be quite complex and the evolution of the coupled parameterized-resolvable scale modeling system appears to be highly nonlinear. However, it may be possible to explain some of the spatial variations in the initial triggering of convection in terms of model initial conditions, such as horizontal variations in moisture. For example, initial conditions are very moist over most of Kansas and northern Oklahoma, but dry out rapidly to the south and west (see Zhang et al., 1989). As simulated surface insolation is applied during the model integration, conditional instability develops over a large area. However, the

amount of lifting required for parcels to reach their LFC is considerably less over the moister regions than over the dry ones. Consequently, those trigger functions that incorporate some measure of the thickness of the layer or negative area between the incipient updraft mixture and its level of free convection (i.e., the LDT and NAT formulations) result in a dearth of parameterized convection over the relatively dry regions. As a further consequence of this tendency, the onset of convection in association with the advancing large-scale forcing is apparently delayed when the NAT is used and missed entirely when the LDT is used, introducing considerable forecast errors in these squall line simulations. In contrast, the timing of the squall line with the FCT and AKT formulations appears to be much more accurate, apparently because these triggering mechanisms are less strongly influenced by the height difference between the mixture and its LFC. Specifically, recall that the FCT implicitly assumes a parcel can reach its LCL and it checks mixed parcel buoyancy at that level. For the AKT, the negative area near cloud base is not likely to strongly inhibit convection in this particular case because the positive area happens to be so large. These results are not sufficient to imply that the FCT and AKT formulations are generally superior, however. For example, in the present case, improved timing of the squall line appears to have been captured at the expense of a more cohesive structure when the AK and FC triggers are used, since convection develops over a significant area where it was not observed to have occurred.

Furthermore, this simulation is sensitive not only to the specific trigger function formulation, but to the imposed values of functional parameters within a given formulation as well. For example, experiments with the AKT suggest that a particular threshold value of moisture convergence is not likely to be generally applicable. The magnitude of moisture convergence in a column is almost certainly strongly dependent upon such factors as model grid resolution and ambient specific humidity. Moreover, additional tests (not shown) indicate that varying the specified lifting depth of the LDT from 50 to 250 hPa, or the  $k$  value of the NAT from 10 to 100, introduces at least as much variability into the results of this case as does the use of completely different formulations.

In general, implementation of unrealistic thresh-

old values or parameters in a given trigger function can have serious detrimental effects on model forecasts. For example, if convection is initiated when mass or moisture convergence exceeds some specified threshold value, it is likely that convection will be activated too soon (late) if the threshold value is prescribed to be too low (high). In the case of a squall line simulation, this raises the possibility that the parameterization might move the line systematically too fast or too slow. If the threshold value is exceedingly high, it is possible that the line might not form at all, or that it might dissipate prematurely. If the threshold value is exceedingly low, spurious convection may develop and disrupt the model's capacity to focus and organize convective activity. Thus, it is evident that erroneous threshold trigger functions may be, at a minimum, a source of phase errors and, in the worst-case scenario, a vehicle whereby the main convective event may be completely missed.

Trigger function sensitivity is likely to be case-dependent. For example, in situations where forcing by the resolvable scale is strong and sharply defined, a triggering mechanism that is directly linked to resolvable scale tendencies may not be susceptible to significant phase errors. However, in situations where resolvable scale forcing is weak over a broad area where convective available potential energy is relatively large, forcing produced by the convection itself (e.g., lifting by moist downdraft outflows) may play a dominant role in shaping the evolution of events. Under these circumstances, the timing and spatial distribution of convective activity can be critically important and weaknesses in the trigger function formulation are likely to lead to more significant forecast errors.

Finally, the sensitivities presented here are meant to heighten awareness of the pivotal role played by the convective trigger function, and to suggest some potentially important considerations for a more general formulation. However, techniques for parameterizing convective initiation are likely to be significantly improved only when the operative physical processes become better understood. Accordingly, it is recommended that continued investigation of this problem not be limited to mesoscale numerical modeling studies. For example, observational examination of convective triggering mechanisms should be included as an objective for upcoming field programs related to the study of deep convection; numerical investigation of these

mechanisms should be performed with cloud-scale numerical models. Without the development of more generally reliable parameterizations of convective initiation, the convective trigger function may become a limiting factor in the continued improvement of operational forecasts of mesoscale convective systems.

#### Acknowledgements

We thank George S. Young for sharing his ideas on trigger function formulations and David J. Stensrud for his helpful comments and supporting numerical simulations. We are grateful to Da-Lin Zhang for providing us with initial conditions for these simulations. We are also grateful to Da-Lin Zhang, Richard H. Johnson, and Steven A. Rutledge for providing supporting figures for this case. The computations were performed on NCAR's CRAY Y-MP. This work was supported by National Science Foundation Grants ATM-87-11014 and ATM-90-24434.

#### References

- Anthes, R. A., 1977: A cumulus parameterization scheme utilizing a one-dimensional cloud model. *Mon. Wea. Rev.*, **105**, 270–286.
- Arakawa, A., Schubert, W. H., 1974: Interaction of a cumulus cloud ensemble with the large-scale environment, Part I. *J. Atmos. Sci.*, **31**, 674–701.
- Anthes, R. A., Hsie, E.-Y., Kuo, Y. H., 1987: *Description of the Penn State/NCAR Mesoscale Model Version 4 (MM4)*, NCAR/TN-282 + STR, National Center for Atmospheric Research, Boulder, CO, 66 pp.
- Bean, B. R., Emmanuel, C. B., Gilmer, R. O., McGavin, R. E., 1975: The spatial and temporal variations of the turbulent fluxes of heat, momentum and water vapor over Lake Ontario. *J. Phys. Oceanogr.*, **5**, 532–540.
- Bean, B. R., Gilmer, R., Grossman, R. L., McGavin, R., 1972: An analysis of airborne measurements of vertical water vapor flux during BOMEX. *J. Atmos. Sci.*, **29**, 860–869.
- Blackadar, A. K., 1979: High resolution models of the planetary boundary layer. In: Pfafflin, J., Ziegler, E. (eds.) *Advances in Environmental Science and Engineering*, 1, No. 1. New York: Gordon and Breach Sci. Publ., 50–85.
- Chen, C., Orville, H. D., 1981: Effects of mesoscale convergence on cloud convection. *J. Appl. Meteor.*, **19**, 256–274.
- Cunning, J. B., 1986: The Oklahoma-Kansas preliminary regional experiment for STORM-Central. *Bull. Amer. Soc.*, **67**, 1478–1486.
- Dudhia, J., 1989: Numerical study of convection observed during the winter monsoon experiment using a mesoscale two-dimensional model. *J. Atmos. Sci.*, **46**, 3077–3107.
- Frank, W. M., Cohen, C., 1985: Properties of tropical cloud ensembles estimated using a cloud model and an observed updraft population. *J. Atmos. Sci.*, **42**, 1911–1928.
- Fritsch, J. M., Chappell, C. F., 1980: Numerical prediction of convectively driven mesoscale pressure systems. Part I: Convective parameterization. *J. Atmos. Sci.*, **37**, 1722–1733.
- Fritsch, J. M., Chappell, C. F., Hoxit, L. R., 1976: The use of

- large-scale budgets for convective parameterization. *Mon. Wea. Rev.*, **104**, 1408–1418.
- Grell, G. A., 1992: Prognostic evaluation of assumptions used by cumulus parameterizations. *Mon. Wea. Rev.* (in press).
- Johnson, R. H., Hamilton, P. J., 1988: The relationship of surface pressure features to the precipitation and air flow structure of an intense midlatitude squall line. *Mon. Wea. Rev.*, **116**, 1444–1472.
- Kain, J. S., Fritsch, J. M., 1990: A one-dimensional entraining/detraining plume model and its application in convective parameterization. *J. Atmos. Sci.*, **47**, 2784–2802.
- Kreitzberg, C. W., Perkey, D. J., 1976: Release of potential instability: Part I. A sequential plume model within a hydrostatic primitive equation model. *J. Atmos. Sci.*, **33**, 456–475.
- Kuo, H. L., 1974: Further studies of the parameterization of the influence cumulus convection on large scale flow. *J. Atmos. Sci.*, **31**, 1232–1240.
- Rutledge, S. A., Houze, R. A., Biggerstaff, M. I., Matejka, T., 1988: The Oklahoma-Kansas convection system of 10–11 June 1985: Precipitation structure and single-doppler radar analysis. *Mon. Wea. Rev.*, **116**, 1409–1430.
- Stull, R. B., 1988: *An Introduction to Boundary Layer Meteorology*. Dordrecht: Kluwer Academic Publishers, 666 pp.
- Young, G., Fritsch, J. M., 1989: A proposal for general convections in analysis of mesoscale boundaries. *Bull. Amer. Meteor. Soc.*, **70**, 1412–1421.
- Zhang, D.-L., Anthes, R. A., 1982: A high resolution model of the planetary boundary layer—sensitivity tests and comparisons with SESAME-79 data. *J. Appl. Meteor.*, **21**, 1594–1609.
- Zhang, D.-L., Chang, H.-R., Seaman, N. L., Warner, T. T., Fritsch, J. M., 1986: A two-way interactive nesting procedure with variable terrain resolution. *Mon. Wea. Rev.*, **114**, 1330–1339.
- Zhang, D.-L., Fritsch, J. M., 1986: Numerical simulation of the meso- $\beta$  scale structure and evolution of the 1977 Johnstown flood. Part I: Model description and verification. *J. Atmos. Sci.*, **43**, 1913–1943.
- Zhang, D.-L., 1989: The effect of parameterized ice microphysics on the simulation of vortex circulation with a mesoscale hydrostatic model. *Tellus*, **41A**, 132–147.
- Zhang, D.-L., Gao, K., 1989: Numerical simulation of an intense squall line during 10–11 June 1985 PRE-STORM. Part II: Rear inflow, surface pressure perturbations, and stratiform precipitation. *Mon. Wea. Rev.*, **117**, 2067–2094.
- Zhang, D.-L., Gao, K., Parsons, D. B., 1989: Numerical simulation of an intense squall line during 10–11 June 1985 PRE-STORM. Part I: Model verification. *Mon. Wea. Rev.*, **117**, 960–994.

Authors' address: J. S. Kain and J. M. Fritsch, Department of Meteorology, 503 Walker Building, The Pennsylvania State University, University Park, PA 16802, U.S.A.